Apparent stiffening of a graphene nanomembrane with initial curvature

Drozdov, A. D.; Christiansen, J. de Claville

Published in:
A I P Advances

DOI (link to publication from Publisher):
10.1063/1.4982797

Publication date:
2017

Document Version
Publisher's PDF, also known as Version of record

Apparent stiffening of a graphene nanomembrane with initial curvature

A. D. Drozdov, and J. deClaville Christiansen

Citation: AIP Advances **7**, 045123 (2017);
View online: https://doi.org/10.1063/1.4982797
View Table of Contents: http://aip.scitation.org/toc/adv/7/4
Published by the American Institute of Physics

Apparent stiffening of a graphene nanomembrane with initial curvature

A. D. Drozdov[a] and J. deClaville Christiansen
Department of Materials and Production, Aalborg University, Fibigerstraede 16, Aalborg 9220, Denmark

(Received 8 December 2016; accepted 18 April 2017; published online 27 April 2017)

A model is developed for bending of a suspended nanomembrane with account for interaction between in-plane and out-of-plane deformation modes. It is shown that the maximum deflection of an initially flat nanomembrane exceeds strongly that of the nanomembrane with an initial curvature. The effect of defects in the crystalline structure of a graphene monolayer on deflection of an initially curved nanomembrane is studied numerically. [http://dx.doi.org/10.1063/1.4982797]

I. INTRODUCTION

Experimental investigation of mechanical properties of nanomembranes formed by a crystalline monolayer or a few layers bridged by adhesion forces has attracted substantial attention in the past decade, see observations on graphene,[1–3] graphene oxide,[4,5] reduced graphene oxide,[6] molybdenum disulfide,[7] bismuth telluride,[8] bismuth selenide,[8] and tungsten selenide,[9] to mention a few. The importance of accurate measurements of elastic moduli is explained by the ability of in-plane strains to modulate electronic band gaps of heterostructures formed by stacks of nanosheets.[10,11]

In mechanical tests, a membrane with thickness h (of order of 1 nm) is suspended over a cylindrical cavity with radius a (of order of several μm). Afterwards, a uniform pressure q (or a concentrated force P in the center) is applied. Deformation of the membrane under load is characterized by its maximum deflection W (of order of tens to hundreds of nm). Presuming bending to be described within the Foppl–von Karman model in the membrane regime, the effective deflection $\delta = W - W_0$, where W_0 denotes the maximum deflection before loading, is expressed in terms of the external force (q or P) by means of the approximate equations[12]

$$q = 4\frac{\sigma_0}{a}\left(\frac{\delta}{a}\right) + \frac{8E}{3(1-\nu)a}\left(\frac{\delta}{a}\right)^3, \qquad P = \pi\sigma_0 a\left(\frac{\delta}{a}\right) + Ea\left(f\frac{\delta}{a}\right)^3 \tag{1}$$

where σ_0 stands for the prestress in the membrane (in-plane tension with the dimension N/m), E is the 2D elastic modulus (with the dimension N/m), and the coefficient f is a dimensionless function of Poisson's ratio ν with the conventional approximation $f = (1.049 - 0.146\nu - 0.158\nu^2)^{-1}$.

Eqs. (1) are asymptotically correct when two conditions are satisfied:[13] (i) the energy of out-of-plane bending is small compared with the energy of in-plane stretching, and (ii) the prestress is small compared with the external load. For a circular membrane under uniform pressure these conditions read $Eh^3 \ll qa^4$ and $\sigma_0^3 \ll E(qa)^2$. Although the above inequalities are fulfilled in bending tests on nanomembranes, treatment of experimental data reveals a counter-intuitive stiffening (an apparent increase in the elastic modulus) of a monolayer membrane induced by the growth of concentration of point and linear defects under ion bombardment,[14] which contradicts the conventional viewpoint that defects in a crystalline lattice induce softening of its elastic response.[15–18]

[a]E–mail: aleksey@m-tech.aau.dk. Phone: +45 41 30 45 04

The defect-induced stiffening of a suspended membrane may be attributed to the fact that the membrane is not flat before loading, but contains a number of wrinkles and ripples.[19] The presence of wrinkles and ripples in 2D nanomembranes is confirmed by observations reported in Refs. 4, 20, 21, to mention a few. According to, Ref. 22 an increase in concentration of point defects under irradiation results in (i) a reduction of the in-plane elastic modulus and (ii) an increase in the initial out-of-plane deflection of a defective lattice. It can also lead to development of in-plane strains in a nanomembrane.[23] The account for initial deflection contradicts, however, Eqs. (1) that are grounded on the assumption that the out-of-plane bending energy of a nanomembrane is negligible compared with the energy of in-plane stretching. The objective of this study is to demonstrate that (i) the force–deflection diagram of a nanomembrane is strongly affected by its initial curvature even under the classical assumption that the bending rigidity is negligible compared with a properly normalized Young's modulus, and (ii) the growth of the initial curvature of a monolayer membrane may explain its apparent stiffening reported in Ref. 14.

II. MODEL

For definiteness, we focus on cylindrical bending of a nanomembrane with clamped edges suspended over a trench with width l under the action of uniform pressure q (this setup was studied experimentally in Refs. 5 and 24). To simplify the analysis, we disregard prestress in the membrane and presume its deformation to depend on longitudinal coordinate x only. The mechanical energy per unit width of a rectangular membrane reads[25]

$$U = \int_{-\frac{l}{2}}^{\frac{l}{2}} \frac{1}{2} E\epsilon^2 \mathrm{d}x + \int_{-\frac{l}{2}}^{\frac{l}{2}} \frac{1}{2} D(\kappa - \kappa_0)^2 \mathrm{d}x, \tag{2}$$

where D is the bending rigidity with the dimension N·m,

$$\epsilon = \frac{\mathrm{d}u}{\mathrm{d}x} + \frac{1}{2}\Big(\frac{\mathrm{d}w}{\mathrm{d}x}\Big)^2 \tag{3}$$

denotes tensile strain, $\kappa = \mathrm{d}^2 w/\mathrm{d}x^2$ stands for the curvature of the membrane, and u, w are the in-plane and out-of plane displacements that satisfy the boundary conditions

$$u\Big(\pm\frac{l}{2}\Big) = 0, \qquad w\Big(\pm\frac{l}{2}\Big) = 0. \tag{4}$$

The novelty of our approach consists in the explicit account for the initial curvature κ_0 in Eq. (2). This quantity is treated as a constant, and it serves as a measure of initial deflection of a nanomembrane suspended on a substrate. The influence of ripples and wrinkles in a suspended membrane is disregarded as the maximum initial deflection exceeds their amplitude by at least an order of magnitude.[4]

As it is commonly accepted for nanomembranes,[26] E and D are treated as independent parameters that obey the condition

$$\varepsilon = \Big(\frac{D}{ql^3}\Big)^{\frac{1}{2}} \Big(\frac{ql}{E}\Big)^{\frac{1}{6}} \ll 1. \tag{5}$$

Equating the rate of changes in the mechanical energy U to the work produced by pressure q per unit time and unit width, we arrive at (i) the stress–strain relation

$$\sigma = E\epsilon, \tag{6}$$

where σ stands for the in-plane stress (tensile force) in the membrane, (ii) the equilibrium equations

$$\frac{\mathrm{d}\sigma}{\mathrm{d}x} = 0, \qquad D\frac{\mathrm{d}^4 w}{\mathrm{d}x^4} - \sigma\frac{\mathrm{d}^2 w}{\mathrm{d}x^2} = q, \tag{7}$$

and (iii) the boundary condition

$$\frac{\mathrm{d}^2 w}{\mathrm{d}x^2}\Big(\pm\frac{l}{2}\Big) = -K \tag{8}$$

with $K = -\kappa_0$. Eqs. (7) and (8) imply that for a positive κ_0, the initial shape of the membrane is concave, in accord with AFM images reported in Refs. 4,12,14,20,21,24.

It follows from the first equation in Eq. (7) that the stress σ is independent of x. The solution of the other equation in Eq. (7) with boundary conditions (4) and (8) is given by

$$w = \frac{K}{\mu^2} + \frac{ql^2}{\sigma}\Big(\frac{1}{8} - \frac{x^2}{2l^2} - \frac{1}{(\mu l)^2}\Big) + \Big(\frac{q}{\sigma} - K\Big)\frac{\cosh(\mu x)}{\mu^2\cosh(\frac{\mu l}{2})} \tag{9}$$

with

$$\mu = \sqrt{\frac{\sigma}{D}}. \tag{10}$$

According to Eq. (9), the maximum deflection of the membrane $W = w(0)$ reads

$$W = \frac{l^2}{8}\Big\{\frac{q}{\sigma}\Big[1 - \Big(\frac{\sinh(\frac{z}{4})}{\frac{z}{4}}\Big)^2\frac{1}{\cosh(\frac{z}{2})}\Big] + \frac{K}{\cosh(\frac{z}{2})}\Big(\frac{\sinh(\frac{z}{4})}{\frac{z}{4}}\Big)^2\Big\}, \tag{11}$$

where $z = \mu l$. It follows from Eqs. (3) and (6) that

$$\frac{du}{dx} + \frac{1}{2}\Big(\frac{dw}{dx}\Big)^2 = \frac{\sigma}{E}.$$

Integration of this equation with the boundary condition (4) results in

$$\sigma = \frac{E}{2l}\int_{-\frac{l}{2}}^{\frac{l}{2}}\Big(\frac{dw}{dx}\Big)^2 dx. \tag{12}$$

Combination of Eqs. (9) and (12) yields

$$\sigma = El^2\Big(\frac{q}{\sigma}\Big)^2\Big\{\Big[\frac{1}{24} + \frac{1}{4z^2\cosh^2(\frac{z}{2})}\Big(\frac{\sinh(z)}{z} - 1\Big) + \frac{1}{z^2}\Big(\frac{\tanh(\frac{z}{2})}{\frac{z}{2}} - 1\Big)\Big]$$
$$- \frac{K\sigma}{q}\Big[\frac{1}{2z^2\cosh^2(\frac{z}{2})}\Big(\frac{\sinh(z)}{z} - 1\Big) + \frac{1}{z^2}\Big(\frac{\tanh(\frac{z}{2})}{\frac{z}{2}} - 1\Big)\Big] + \frac{K^2\sigma^2}{4q^2z^2\cosh^2(\frac{z}{2})}\Big(\frac{\sinh(z)}{z} - 1\Big)\Big\}.$$

Using Eqs. (5), (10), we present this equation as follows:

$$(\varepsilon z)^6 = F_1(z) - \frac{D}{ql^3}(Kl)F_2(z) + \frac{1}{4}\Big(\frac{D}{ql^3}\Big)^{\frac{3}{2}}\Big(\frac{E}{ql}\Big)^{\frac{1}{6}}(Kl)^2(\varepsilon z)F_3(z) \tag{13}$$

with

$$F_1(z) = \frac{1}{24} + \frac{1}{4z^2\cosh^2(\frac{z}{2})}\Big(\frac{\sinh(z)}{z} - 1\Big) + \frac{1}{z^2}\Big(\frac{\tanh(\frac{z}{2})}{\frac{z}{2}} - 1\Big),$$
$$F_2(z) = \frac{1}{2\cosh^2(\frac{z}{2})}\Big(\frac{\sinh(z)}{z} - 1\Big) + \Big(\frac{\tanh(\frac{z}{2})}{\frac{z}{2}} - 1\Big),$$
$$F_3(z) = \frac{1}{\cosh^2(\frac{z}{2})}\Big(\sinh(z) - \frac{1}{z^2}\Big).$$

We search for a solution of Eq. (13) in the form

$$z = \frac{1}{\varepsilon}(b_0 + b_1\varepsilon + b_2\varepsilon^2 + \ldots), \tag{14}$$

where b_m are coefficients to be found. Substitution of expression (14) into Eq. (13) implies that b_0 is a solution of the nonlinear equation

$$b_0^6 = \frac{1}{24} + \frac{D}{ql^3}(Kl) + \frac{1}{4}\Big(\frac{D}{ql^3}\Big)^{\frac{3}{2}}\Big(\frac{E}{ql}\Big)^{\frac{1}{6}}(Kl)^2 b_0. \tag{15}$$

The other coefficients in Eq. (14) are determined in a similar manner by using the Maclaurin expansions of the functions $F_m(z)$ at $z = \infty$.

Eqs. (10) and (11) imply that the maximum deflection of the membrane reads

$$W = \frac{ql^4}{8Dz^2}\Big\{\Big[1 - \Big(\frac{\sinh(\frac{z}{4})}{\frac{z}{4}}\Big)^2 \frac{1}{\cosh(\frac{z}{2})}\Big] + 8\frac{D}{ql^3}(Kl)\Big[1 - \frac{1}{\cosh(\frac{z}{2})}\Big]\Big\}.$$

Inserting expression (14) into this equality and taking the limit as $\varepsilon \to 0$, we find that

$$\frac{W}{l} = \frac{1}{8b_0^2}\Big(\frac{ql}{E}\Big)^{\frac{1}{3}}\Big[1 + 8\frac{D}{ql^3}(Kl)\Big]. \tag{16}$$

When $K = 0$, Eqs. (15) and (16) result in the conventional formula

$$\tilde{W} = \tilde{q}^{\frac{1}{3}}, \tag{17}$$

where $\tilde{W} = W/W_*$, $\tilde{q} = q/q_*$, and the characteristic deflection W_* is connected with the characteristic pressure q_* by the formula

$$\frac{W_*}{l} = \frac{1}{4}\Big(\frac{3q_*l}{E}\Big)^{\frac{1}{3}}. \tag{18}$$

In the general case $K > 0$, Eqs. (15) and (16) yield

$$\tilde{W} = \frac{1}{2b_0^2}\Big(\frac{\tilde{q}}{3}\Big)^{\frac{1}{3}}\Big(1 + \frac{8Z}{\tilde{q}}\Big), \qquad b_0^6 = \frac{1}{24} + \frac{Z}{\tilde{q}} + \frac{3^{\frac{1}{6}}AZ^{\frac{3}{2}}}{8\tilde{q}^{\frac{5}{3}}}b_0 \tag{19}$$

with

$$A = 2\Big(\frac{E}{3q_*l}\Big)^{\frac{1}{6}}(Kl)^{\frac{1}{2}}, \qquad Z = \frac{D}{q_*l^3}(Kl). \tag{20}$$

III. NUMERICAL SIMULATION

Given A and Z, Eq. (19) is solved by the Newton-Raphson method. Results of simulation are depicted in Figures 1 and 2, where the dimensionless maximum deflection $\tilde{\delta} = \tilde{W} - \tilde{W}_0$ ($\tilde{W}_0$ stands for $\tilde{W}$ at $\tilde{q} = 0$) is plotted versus dimensionless pressure $\tilde{q}$. These figures show that for a fixed $\tilde{q}$, $\tilde{\delta}$ decreases monotonically with Z (which means that the growth of initial curvature K results in an apparent stiffening of a membrane). For a given Z, the reduction in $\tilde{\delta}$ is weakened with an increase in A, that is with the growth of elastic modulus E. In simulation, parameter Z is changed in a rather wide interval because the bending rigidities of a graphene monolayer D determined by means of

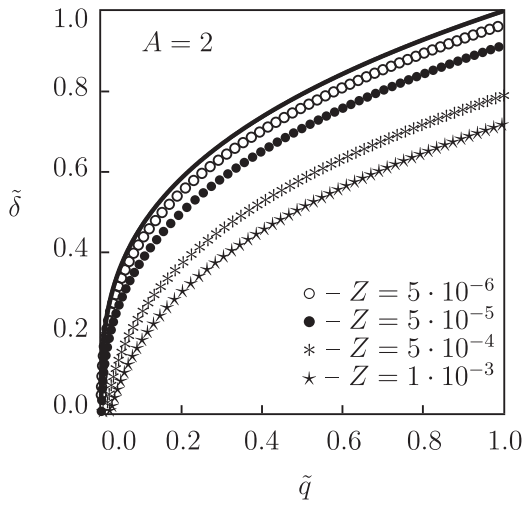

FIG. 1. Maximum deflection $\tilde{\delta}$ versus pressure $\tilde{q}$. Solid line: solution of Eq. (17). Symbols: results of simulation with $A = 2$ and various Z.

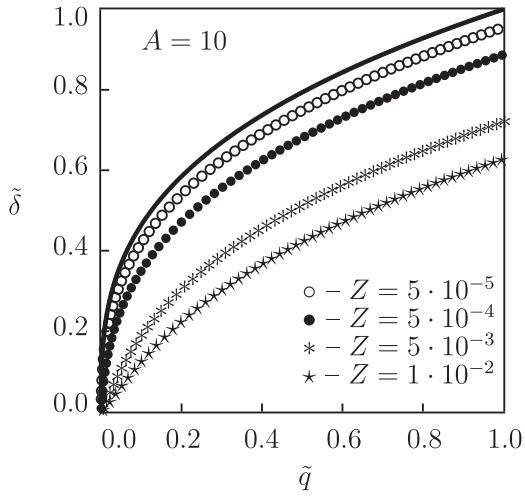

FIG. 2. Maximum deflection $\tilde{\delta}$ versus pressure $\tilde{q}$. Solid line: solution of Eq. (17). Symbols: results of simulation with $A = 10$ and various Z.

the density functional theory (0.83 to 1.62 eV) and calculated within the Kirchhoff model (22.3 eV) differ by more than an order of magnitude.[25]

Figures 1 and 2 reveal the effect of initial curvature $K = -\kappa_0$ on the maximum deflection of a nanomembrane when the quantities E and D are treated as independent parameters.[26]

To assess how the maximum deflection evolves with elastic modulus when D and E are connected by the conventional relation $D = \frac{1}{12}Eh^2$ (we disregard Poisson's ratio and recall that E stands for the 2D elastic modulus), Eqs. (19), (20) are solved for a monolayer membrane made of reduced graphene oxide with the Young's modulus 0.82 TPa[16] and thickness $h = 1.2$ nm[27] suspended over a trench with width $l = 1$ μm (this value equals the diameter of a circular membrane used in experiments[16]). We set $q_* = 0.02$ MPa and determine the initial curvature from the formula for a circular segment $K = 8W_0/(l^2 + 4W_0^2)$, where the maximum deflection before application of pressure reads $W_0 = 20$ nm in accord with Ref. 4.

Evolution of the maximum deflection $\tilde{\delta}$ with pressure $\tilde{q}$ is illustrated in Figure 3, where results of simulation are depicted for a non-damaged membrane with $K = 0$, a non-damaged membrane with the non-zero initial curvature K, and damaged membranes with the non-zero K (to account for creation of

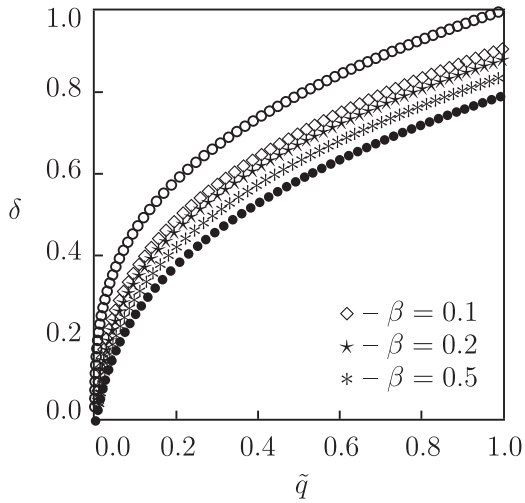

FIG. 3. Maximum deflection $\tilde{\delta}$ versus pressure $\tilde{q}$. Unfilled circles: undamaged membrane with the zero initial curvature. Filled circles: undamaged membrane with the non-zero initial curvature. Other symbols: damaged membrane with the non-zero initial curvature and various degrees of damage β.

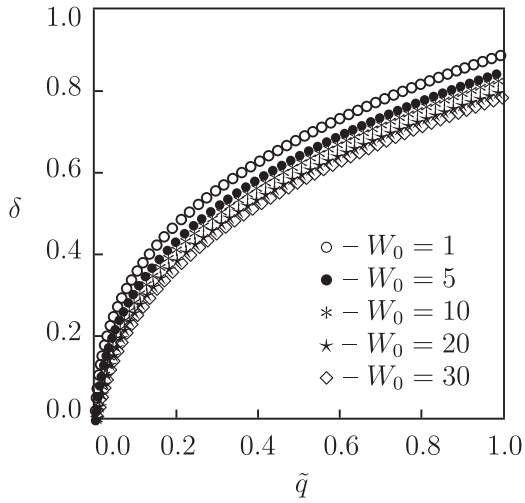

FIG. 4. Maximum deflection δ versus pressure $\tilde{q}$. Symbols: results of simulation for a damaged membrane with $\beta = 0.9$ and various maximum initial deflections W_0 nm.

defects, the Young's modulus E is replaced with βE, where $\beta = 0.1$, 0.2, and 0.5). It is worth noting the coincidence of our results with those reported in Ref. 14: the maximum deflection of the damaged membrane with $\beta = 0.5$ equals 0.82 of that of the non-damaged membrane with the zero initial curvature. Figure 3 demonstrates that for each pressure $\tilde{q}$ under consideration, the maximum deflection $\tilde{\delta}$ is reduced substantially due to the presence of initial curvature (the latter is observed as an apparent stiffening). Damage induced by irradiation results in weakening of the membrane (an increase in its maximum deflection $\tilde{\delta}$). However, even when the membrane with a non-zero K is severely damaged ($\beta = 0.1$), its maximum deflection remains lower than that of a non-damaged membrane with $K = 0$.

To assess the effect of initial curvature on the maximum deflection of a nanomembrane, Eqs. (19) and (20) are solved numerically with the above parameters for a weakly damaged membrane ($\beta = 0.9$) with various initial deflections W_0 ranging from 1 to 30 nm. Results of simulation are depicted in Figure 4 which demonstrates that an increase in the initial curvature K leads to a reduction in the maximum deflection $\tilde{\delta}$ for all dimensionless pressures $\tilde{q}$.

IV. CONCLUSIONS

A simple model is developed for the analysis of cylindrical bending of a nanomembrane that takes into account interaction between in-plane and out-of-plane deformation modes. The in-plane elastic modulus E and bending rigidity D are treated as independent parameters that obey condition (5). An advantage of the proposed approach is that it allows bending of a nanomembrane with an initial curvature to be evaluated by means of semi-analytical Eq. (19) with only two parameters A and Z.

The effect of initial curvature on the maximum deflection of a membrane is studied numerically. It is demonstrated that an increase in initial deflection (within the range observed in experiments) induces a pronounced decay in the maximum deflection of a nanomembrane under pressure. Results of simulation show that the maximum deflection of an initially flat monolayer membrane with the 2D elastic modulus E exceeds that of an initially curved membrane with a smaller modulus βE, where $\beta < 1$ accounts for damage in the crystalline structure of a graphene monolayer caused by formation of defects.

ACKNOWLEDGMENTS

Financial support by the Danish Innovation Fund (project 5152–00002B) is gratefully acknowledged.

[1] C. Lee, X. Wei, J. W. Kysar, and J. Hone, Science **321**, 385–388 (2008).
[2] S. P. Koenig, N. G. Boddeti, M. L. Dunn, and J. S. Bunch, Nat. Nanotechnol. **6**, 543–546 (2011).
[3] R. J. T. Nicholl, H. J. Conley, N. V. Lavrik, I. Vlassiouk, Y. S. Puzyrev, V. P. Sreenivas, S. T. Pantelides, and K. I. Bolotin, Nat. Comm. **6**, 8789 (2015).
[4] J. W. Suk, R. D. Piner, J. An, and R. S. Ruoff, ACS Nano **4**, 6557–6564 (2010).
[5] N. Sridi, B. Lebental, J. Azevedo, J. C. P. Gabriel, and A. Ghis, Appl. Phys. Lett. **103**, 051907 (2013).
[6] C. Gomez-Navarro, M. Burghard, and K. Kern, Nano Lett. **8**, 2045–2049 (2008).
[7] D. Lloyd, X. Liu, J. W. Christopher, L. Cantley, A. Wadehra, B. L. Kim, B. B. Goldberg, A. K. Swan, and J. S. Bunch, Nano Lett. **16**, 5836–5841 (2016).
[8] H. Yan, C. Vajner, M. Kuhlman, L. Guo, L. Li, P. T. Araujo, and H.-T. Wang, Appl. Phys. Lett. **109**, 032103 (2016).
[9] R. Zhang, V. Koutsos, and R. Cheung, Appl. Phys. Lett. **108**, 042104 (2016).
[10] A. K. Geim and I. V. Grigorieva, Nature **499**, 419–425 (2013).
[11] R. Roldan, A. Castellanos-Gomez, E. Cappelluti, and F. Guinea, J. Phys.: Condens. Matter **27**, 313201 (2015).
[12] A. Castellanos-Gomez, V. Singh, H. S. J. van der Zant, and G. A. Steele, Ann. Phys. **527**, 27–44 (2015).
[13] M. R. Begley and T. J. Mackin, J. Mech. Phys. Solids **52**, 2005–2023 (2004).
[14] G. Lopez-Polin, C. Gomez-Navarro, V. Parente, F. Guinea, M. I. Katsnelson, F. Perez-Murano, and J. Gomez-Herrero, Nat. Phys. **11**, 26–31 (2015).
[15] F. Hao, D. Fang, and Z. Xu, Appl. Phys. Lett. **99**, 041901 (2011).
[16] A. Zandiatashbar, G.-H. Lee, S. J. An, S. Lee, N. Mathew, M. Terrones, T. Hayashi, C. R. Picu, J. Hone, and N. Koratkar, Nat. Comm. **5**, 3186 (2014).
[17] K. Liu, C.-L. Hsin, D. Fu, J. Suh, S. Tongay, M. Chen, Y. Sun, A. Yan, J. Park, K. M. Yu, W. Guo, A. Zettl, H. Zheng, D. C. Chrzan, and J. Wu, Adv. Mater. **27**, 6841–6847 (2015).
[18] J. Martinez-Asencio, C. J. Ruestes, E. M. Bringa, and M. J. Caturla, Phys. Chem. Chem. Phys. **18**, 13897–13903 (2016).
[19] C. S. Ruiz-Vargas, H. L. Zhuang, P. Y. Huang, A. M. van der Zande, S. Garg, P. L. McEuen, D. A. Muller, R. G. Hennig, and J. Park, Nano Lett. **11**, 2259–2263 (2011).
[20] C.-L. Wong, M. Annamalai, Z.-Q. Wang, and M. Palaniapan, J. Micromech. Microeng. **20**, 115029 (2010).
[21] L. Guo, H. Yan, Q. Moore, M. Buettner, J. Song, L. Li, P. T. Araujob, and H.-T. Wang, Nanoscale **7**, 11915–11921 (2015).
[22] Z. Song and Z. Xu, Extreme Mech. Lett. **6**, 82–87 (2016).
[23] N. Blanc, F. Jean, A. V. Krasheninnikov, G. Renaud, and J. Coraux, Phys. Rev. Lett. **111**, 085501 (2013).
[24] N. Lindahl, D. Midtvedt, J. Svensson, O. A. Nerushev, N. Lindvall, A. Isacsson, and E. E. B. Campbell, Nano Lett. **12**, 3526–3531 (2012).
[25] Y. Wei, B. Wang, J. Wu, R. Yang, and M. L. Dunn, Nano Lett. **13**, 26–30 (2013).
[26] E. Gao and Z. Xu, J. Appl. Mech. **82**, 121012 (2015).
[27] J. Zhang, H. Yang, G. Shen, P. Cheng, J. Zhang, and S. Guo, Chem. Commun. **46**, 1112–1114 (2010).